



Center for Aeronautical Research

**Bureau of Engineering Research
 The University of Texas at Austin
 Austin, Texas**

CAR 89-3

**APPLICATION OF ATTACHMENT MODES IN THE
 CONTROL OF LARGE SPACE STRUCTURES**

by

Roy R. Craig, Jr.

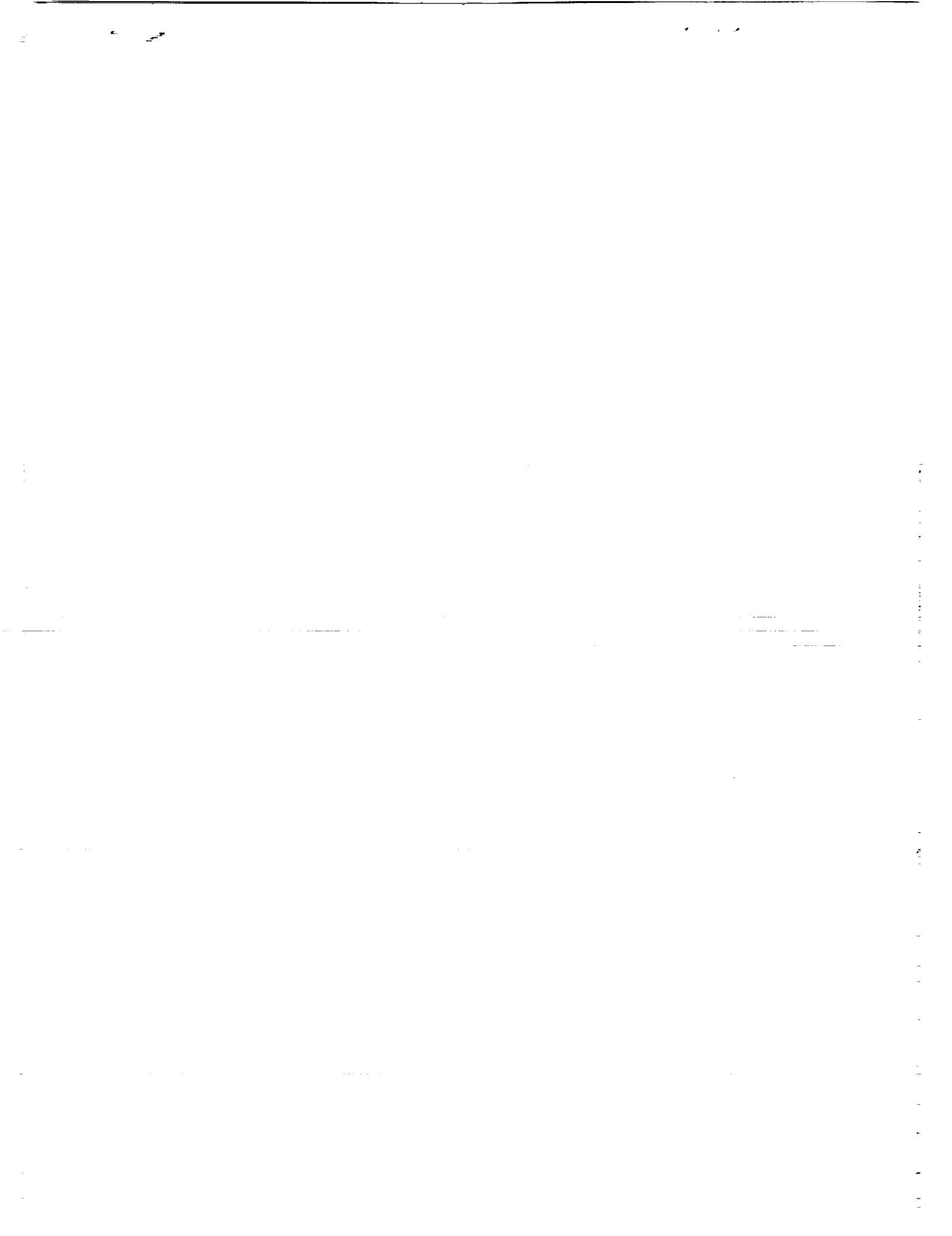
**NASA Contract N^o. NAS9-17254
 September, 1989**

(NASA-CR-185604) APPLICATION OF ATTACHMENT
 MODES IN THE CONTROL OF LARGE SPACE
 STRUCTURES (Texas Univ.) 56 p CSCL 22B

N90-19280

Unclas

G3/18 0271120



APPLICATION OF ATTACHMENT MODES IN THE CONTROL
OF LARGE SPACE STRUCTURES

by
Roy R. Craig, Jr.*

Report No. CAR 89-3

FINAL REPORT

for

NASA Contract NAS9-17254
Lyndon B. Johnson Space Center
Houston, TX

Center for Aeronautical Research
Department of Aerospace Engineering and Engineering Mechanics
Bureau of Engineering Research
College of Engineering
The University of Texas at Austin
Austin, Texas 78712

September, 1989

*Professor, Department of Aerospace Engineering and Engineering Mechanics



ACKNOWLEDGEMENTS

This work was supported by NASA Contract NAS9-17254 with the Lyndon B. Johnson Space Center, Houston, Texas. The interest and support of Dr. George Zupp, Mr. David Hamilton, and Mr. Rodney Rocha during various phases of the work is greatly appreciated.

Appreciation is expressed to Dr. Jeffrey Bennighof for serving as M.S. thesis advisor for Jeffrey Tave. The success of this research project may be credited to the ideas, enthusiasm, and hard work of Russell Turner, Zhenhua Ni, Jeffrey Tave, Hyong Man Kim, and Tzu-Jeng Su.



ABSTRACT

This report covers research conducted during the three phases of the subject contract: Phase 1 (1 Oct. 1984 – 30 June 1986), Phase 2 (1 July 1986 – 10 July 1987), and Phase 3 (11 July 1987 – 1 Sept. 1989). The research, entitled “Application of Attachment Modes in the Control of Large Space Structures,” focussed on various ways to obtain reduced-order mathematical models of structures for use in dynamic response analyses and in controller design studies.

Attachment modes are deflection shapes of a structure subjected to specified unit load distributions. Attachment modes are frequently employed to supplement free-interface normal modes to improve the modeling of components (substructures) employed in component mode synthesis analyses. Deflection shapes of structures subjected to generalized loads of some specified distribution and of unit magnitude can also be considered to be attachment modes. This report summarizes the following papers and reports which were written under this contract:

- Craig, R. R. Jr., “A Review of Time-Domain and Frequency-Domain Component Mode Synthesis Methods,” Ref. [7].
- Craig, R. R. Jr., “A Review of Time-Domain and Frequency-Domain Component Mode Synthesis Methods,” Ref. [8].
- Craig, R. R. Jr. and Hale, A. L., “Block-Krylov Component Synthesis Method for Structural Model Reduction,” Ref. [14].

- Craig, R. R. Jr. and Ni, Z., “Component Mode Synthesis for Model Order Reduction of Non-classically-Damped Systems,” Ref. [15].
- Craig, R. R. Jr., Su, T. J., and Ni, Z., “State Variable Models of Structures Having Rigid-Body Modes,” Ref. [16].
- Kim, H. M. and Craig, R. R. Jr., “System Identification for Large Space Structures,” Ref. [17].
- Kim, H. M. and Craig, R. R. Jr., “Structural Dynamics Analysis Using an Unsymmetric Block Lanczos Algorithm,” Ref. [18].
- Kim, H. M. and Craig, R. R. Jr., “Computational Enhancement of an Unsymmetric Block Lanczos Algorithm,” Ref. [19].
- Turner, R. M. and Craig, R. R. Jr., “Use of Lanczos Vectors in Dynamic Simulation,” Ref. [22].
- Craig, R. R. Jr. and Turner, R. M., “Lanczos Models for Reduced-Order Control of Flexible Structures,” Ref. [23].
- Su, T. J. and Craig, R. R. Jr., “Application of Krylov Vectors and Lanczos vectors to the Control of Flexible Structures,” Ref. [24].
- Su, T. J. and Craig, R. R. Jr., “Model Reduction and Control of Flexible Structures Using Krylov Vectors,” Ref. [25].
- Su, T. J. and Craig, R. R. Jr., “Krylov Model Reduction Algorithm for Undamped Structural Dynamics Systems,” Ref. [26].

- Tave, J. S., Bennighof, J. K., and Craig, R. R. Jr., "A Bilevel Architecture for the Control of Flexible Structures," Ref. [27].

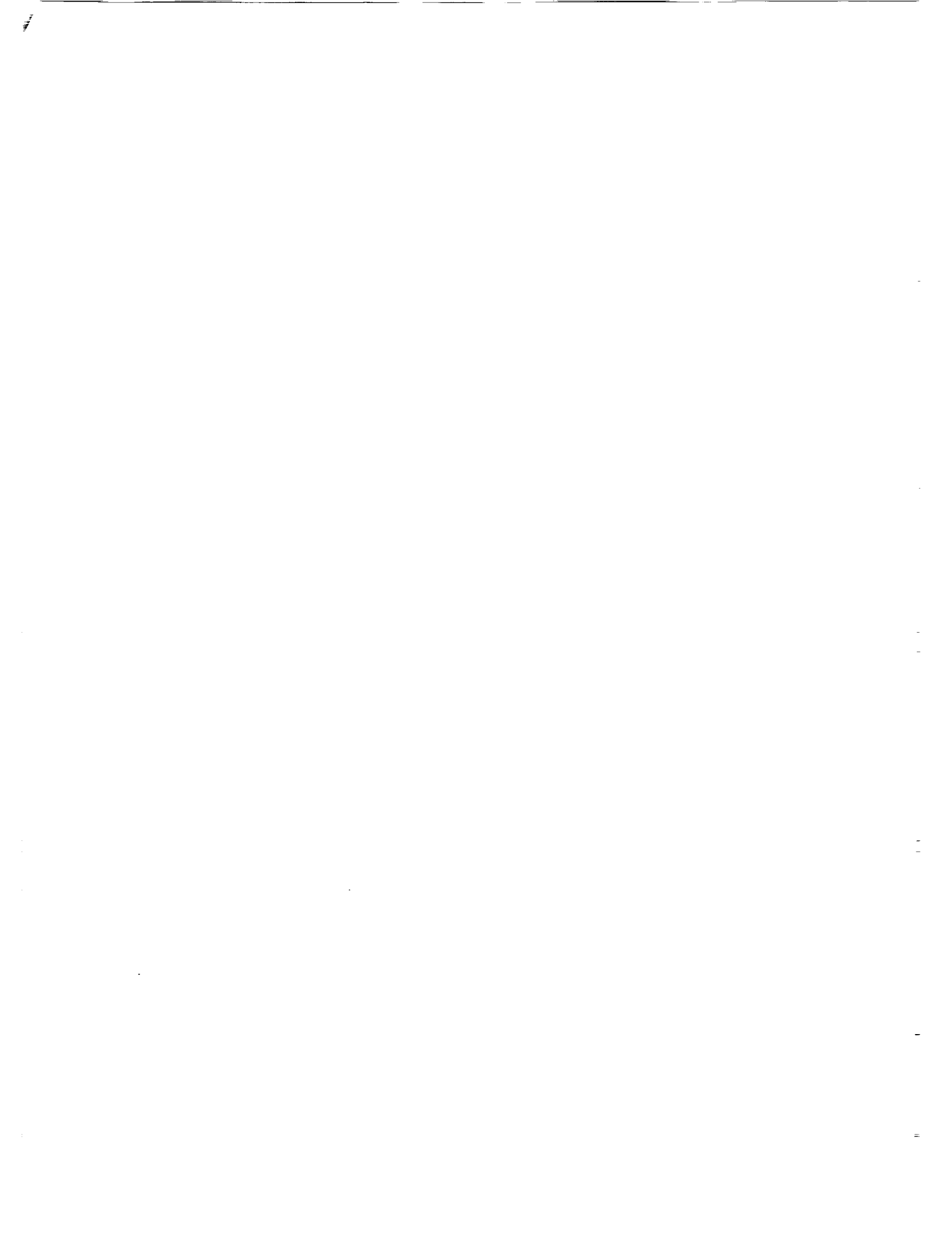


TABLE OF CONTENTS

ACKNOWLEDGEMENTS	ii
ABSTRACT	iii
TABLE OF CONTENTS	vi
1. INTRODUCTION	1
2. SUBSTRUCTURE ANALYSIS METHODS	3
3. USE OF LANCZOS VECTORS IN RESPONSE ANALYSIS AND SYSTEM IDENTIFICATION	13
4. APPLICATION OF KRYLOV VECTORS AND LANCZOS VECTORS TO THE CONTROL OF FLEXIBLE STRUCTURES - PART 1	23
5. APPLICATION OF KRYLOV VECTORS AND LANCZOS VECTORS TO THE CONTROL OF FLEXIBLE STRUCTURES - PART 2	30
6. A BILEVEL ARCHITECTURE FOR THE CONTROL OF FLEXIBLE STRUCTURES	42
7. SUMMARY AND RECOMMENDATIONS	44
BIBLIOGRAPHY	45



1. INTRODUCTION

Attachment modes are deflection shapes of a structure subjected to specified unit load distributions[1]. Attachment modes were originally defined by Bamford as “those modes which result from a concentrated load at a point[2].” This type of attachment mode is frequently employed to supplement free-interface normal modes to improve the free-interface modeling of components (substructures) employed in component mode synthesis analyses[1,3]. Deflection shapes of structures subjected to generalized loads of some specified distribution and of unit magnitude can also be considered to be attachment modes. Reference [4] provides an example of the case of attachment modes defined for distributed loads applied to a structure.

Krylov vectors, and the closely-related Lanczos vectors, constitute a special class of attachment modes. Wilson, et.al.,[5] explored the use of “Ritz vectors” in analyzing the dynamic response of structures. Nour-Omid and Clough[6] described the use of similarly-defined vectors, identifying them as Lanczos vectors. These authors noted the superiority of Lanczos vectors over the usual normal mode vectors as bases for mode superposition solutions of dynamic response problems. The research described in this report was initiated to explore the application of Krylov/Lanczos vectors to the dynamic response of structures and to the control of flexible structures.

This report summarizes various reports and technical papers and presentations which have resulted from the research on applications of various forms of attachment modes. Research related to component mode synthesis

is described in Section 2, followed in Section 3 by a discussion of applications of Lanczos modes in dynamic response analysis and in system identification. The application of Krylov vectors and Lanczos vectors to the control of flexible structures is summarized in Sections 4 and 5. Section 6 summarizes a substructure-based approach to control of flexible structures. Finally, some concluding remarks and recommendations are noted in Section 7.

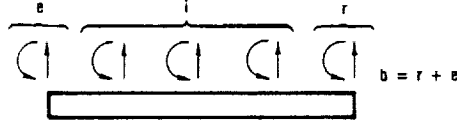
2. SUBSTRUCTURE ANALYSIS METHODS

Since the late 1960's many papers have been published on the topic of component mode synthesis (CMS), or substructure analysis of dynamic response. Very few of these papers treat damped structures, and virtually none treat structures acted upon by general non-conservative forces. In response to an invitation to present an invited paper, and in preparation for extending component mode synthesis methods to structures with arbitrary linear damping, the author compiled an extensive literature review and tutorial article on methods of component mode synthesis[7,8].

In the literature on component mode synthesis there are three basic approaches. One approach employs constraint modes and fixed-interface normal modes, and is typified by the methods of Hurty[9] and of Craig and Bampton[10]. A second approach, which employs attachment modes and free-interface normal modes, is represented by the methods of MacNeal[11] and Rubin[12]. Finally, interface loading is employed by Benfield and Hruda[13]. Two studies related to substructure analysis using attachment modes are described in this Section. Reference [14] describes substructure analysis using a fixed-interface block-Krylov subspace or a free-interface block-Krylov subspace. References [15] and [16] discuss the extension of free-interface component mode synthesis (e.g., Refs. [11], [12], and [3]) to structures having general damping. Figure 1 shows a system composed of components, or substructures, and indicates the loads used to identify interface and non-interface coordinates.



A. COMPONENTS AND COUPLED SYSTEM



B. TYPICAL COMPONENT WITH REDUNDANT BOUNDARY

Figure 1: The component mode synthesis method distinguishes between internal(i) and boundary(b) coordinates. Boundary coordinates are sometimes further divided into rigid-body (r) and excess (e), or redundant coordinates

A *Krylov subspace* of order j is a j -dimensional vector space spanned by columns of the matrix

$$Q_j = [\phi, A\phi, A^2\phi, \dots, A^{(j-1)}\phi] \quad (1)$$

where ϕ is any column vector and A is a square matrix. We have assumed that ϕ is n -dimensional and A is $n \times n$ -dimensional. Depending on the choice of ϕ and A , the basis vectors in Eq. (1) are either linearly dependent for some j less than n or they span the entire n -dimensional space when $j = n$. If ϕ is replaced by a matrix with i columns rather than a single column, the subspace is called a *block-Krylov subspace*.

Reference [14] develops a fixed-interface version and a free-interface version of component mode synthesis for undamped structures using Krylov vectors rather than the usual normal modes. The equation of motion of a component can be written in the following partitioned forms

$$\begin{bmatrix} m_{ii} & m_{ib} \\ m_{bi} & m_{bb} \end{bmatrix} \begin{Bmatrix} \ddot{x}_i \\ \ddot{x}_b \end{Bmatrix} + \begin{bmatrix} k_{ii} & k_{ib} \\ k_{bi} & k_{bb} \end{bmatrix} \begin{Bmatrix} x_i \\ x_b \end{Bmatrix} = \begin{Bmatrix} f_i \\ f_b \end{Bmatrix} \quad (2)$$

$$\begin{bmatrix} m_{ii} & m_{ie} & m_{ir} \\ m_{ei} & m_{ee} & m_{er} \\ m_{ri} & m_{re} & m_{rr} \end{bmatrix} \begin{Bmatrix} \ddot{x}_i \\ \ddot{x}_e \\ \ddot{x}_r \end{Bmatrix} + \begin{bmatrix} k_{ii} & k_{ie} & k_{ir} \\ k_{ei} & k_{ee} & k_{er} \\ k_{ri} & k_{re} & k_{rr} \end{bmatrix} \begin{Bmatrix} x_i \\ x_e \\ x_r \end{Bmatrix} = \begin{Bmatrix} f_i \\ f_e \\ f_r \end{Bmatrix} \quad (3)$$

A *constraint mode* is defined as the static deflection of a structure when a unit displacement is applied to one coordinate of a specified set of coordinates while the remaining coordinates of that set are restrained and the remaining degrees of freedom of the structure are force free. Thus, employing the matrix partitioning of Eq. (2), the set of constraint modes Ψ_c relative to the boundary coordinates, is defined by

$$\begin{bmatrix} k_{ii} & k_{ib} \\ k_{bi} & k_{bb} \end{bmatrix} \begin{bmatrix} \Psi_{ic} \\ I \end{bmatrix} = \begin{bmatrix} 0 \\ R_{bb} \end{bmatrix} \quad (4)$$

That is, Ψ_c is given by

$$\Psi_c = \begin{bmatrix} \Psi_{ic} \\ I \end{bmatrix} = \begin{bmatrix} -k_{ii}^{-1}k_{ib} \\ I \end{bmatrix} \quad (5)$$

In Reference [14] it is shown that a *fixed-interface block-Krylov subspace* for a component may be defined by

$$\Psi_j^c \equiv [\Psi_c^{(0)}, \Psi_c^{(1)}, \Psi_c^{(2)}, \dots, \Psi_c^{(j-1)}] \quad (6)$$

where $\Psi_c^{(0)}$ is given by Eq. (5) and where

$$\Psi_c^{(r)} \equiv \begin{bmatrix} \Psi_{ic}^{(r)} \\ 0 \end{bmatrix} = G_c^r \Psi_c \quad (7)$$

where G_c is defined by

$$G_c = \begin{bmatrix} k_{ii}^{-1}m_{ii} & k_{ii}^{-1}m_{ib} \\ 0 & 0 \end{bmatrix} \quad (8)$$

Then,

$$\Psi_c^{(1)} \equiv \begin{bmatrix} \Psi_{ic}^{(1)} \\ 0 \end{bmatrix} = G_c \Psi_c = \begin{bmatrix} k_{ii}^{-1}(m_{ii}\Psi_{ic} + m_{ib}) \\ 0 \end{bmatrix} \quad (9)$$

and, subsequently,

$$\Psi_c^{(r)} \equiv \begin{bmatrix} k_{ii}^{-1}m_{ii}\Psi_{ic}^{(r-1)} \\ 0 \end{bmatrix}, \quad r = 2, 3, \dots \quad (10)$$

A free-interface analog of Eq. (6) can also be defined. However, this case is complicated by the fact that, when all of the component degrees of freedom are free, the stiffness matrix k will be singular if the component is free to undergo rigid-body motion. In such case, a pseudo-inverse of k is required, and rigid-body modes must be included in the displacement of the component. Using the partitions of Eq. (3), the N_r rigid-body modes can be defined by

$$\begin{bmatrix} k_{ii} & k_{ie} & k_{ir} \\ k_{ei} & k_{ee} & k_{er} \\ k_{ri} & k_{re} & k_{rr} \end{bmatrix} \begin{bmatrix} \Psi_{ir} \\ \Psi_{er} \\ I \end{bmatrix} = \begin{bmatrix} 0 \\ 0 \\ 0 \end{bmatrix} \quad (11)$$

where I is an $r \times r$ unit matrix, and a pseudo-inverse k^{-1} can be defined by

$$k^{-1} = \begin{bmatrix} g_{ii} & g_{ie} & 0 \\ g_{ei} & g_{ee} & 0 \\ 0 & 0 & 0 \end{bmatrix} \quad (12)$$

where

$$\begin{bmatrix} g_{ii} & g_{ie} \\ g_{ei} & g_{ee} \end{bmatrix} = \begin{bmatrix} k_{ii} & k_{ie} \\ k_{ei} & k_{ee} \end{bmatrix}^{-1} \quad (13)$$

An *attachment mode* is defined as the static deflection of a structure when a unit force is applied at one coordinate of a specified set of coordinates, while the remaining unconstrained coordinates are force free. When a structure has rigid-body freedoms, the structure can be restrained at an r -set of coordinates

(Fig. 1), and a set of N_e attachment modes Ψ_a can be defined for unit forces applied at the excess (redundant) coordinates by the equation

$$\begin{bmatrix} k_{ii} & k_{ie} & k_{ir} \\ k_{ei} & k_{ee} & k_{er} \\ k_{ri} & k_{re} & k_{rr} \end{bmatrix} \begin{bmatrix} \Psi_{ia} \\ \Psi_{ea} \\ 0 \end{bmatrix} = \begin{bmatrix} 0 \\ I \\ R_{ra} \end{bmatrix} \quad (14)$$

Let

$$\Psi_b \equiv [\Psi_r \ \Psi_a] \quad (15)$$

where Ψ_r is given by Eq. (11) and Ψ_a by Eq. (14). It is noted in Ref. [14] that Ψ_b spans the same $(N_r + N_e)$ subspace as that spanned by Ψ_c , and it is shown that a *free-interface block-Krylov subspace* of order j may be defined by

$$\Psi_j^b \equiv [\Psi_b^{(0)}, \Psi_b^{(1)}, \Psi_b^{(2)}, \dots, \Psi_b^{(j-1)}] \quad (16)$$

where $\Psi_b^{(0)}$ is given by Eq. (15) and where $\Psi_b^{(r)}$ is given by

$$\Psi_b^{(r)} = G_a^r \Psi_b = G_a \Psi_b^{(r-1)} \equiv k^{-1} m \Psi_b^{(r-1)} \quad (17)$$

Reference [14] proves certain disturbability and observability properties that the block-Krylov subspaces defined by Eqs. (6) and (16) possess. Numerical examples are also provided comparing block-Krylov component synthesis results with results obtained by the Hurty-Craig-Bampton fixed-interface normal mode approach. The accuracy of the fixed-interface block-Krylov method is shown via a numerical example to be comparable to that of fixed-interface component mode synthesis. Since the computational expense of block-Krylov method is less than that for component mode synthesis, the block-Krylov method is preferable.

The block-Krylov substructure methods described above pertain only to undamped structures. A free-interface component mode synthesis method for structures with general damping will be described in the remaining part of this section. This method, which employs complex modes, is described in Refs. [15,16]. An alternative method for treating structures with general damping is discussed in Section 3. The method in Section 3 does not require complex modes.

The equation of motion for a typical free-interface component of a damped structure may be written

$$m\ddot{x} + c\dot{x} + kx = f \quad (18)$$

where m , c , and k are the $(n \times n)$ mass, damping, and stiffness matrices, respectively. There is no assumption that the matrices in Eq. (18) are symmetric, although m and k will normally be symmetric. However, if the component has rigid-body freedom, k will be singular.

Where necessary, Eq. (18) will be expanded into (i, b) partitions or (i, e, r) partitions in accordance with the notation of Figure 1. In this report it will be assumed that there are no external forces acting on the structure, so the only forces exerted on a component act on the boundary, and f has the form

$$f = \begin{Bmatrix} 0_i \\ f_b \end{Bmatrix} \quad (19)$$

Equation (18) can be expanded to $2n$ -order state-space form as follows:

$$A\dot{X} + BX = F \quad (20)$$

where

$$A = \begin{bmatrix} 0 & m \\ m & c \end{bmatrix}, \quad B = \begin{bmatrix} -m & 0 \\ 0 & k \end{bmatrix}, \quad X = \begin{Bmatrix} \dot{x} \\ x \end{Bmatrix}, \quad F = \begin{Bmatrix} 0 \\ f \end{Bmatrix} \quad (21)$$

A and B will be referred to as the state mass matrix and the state stiffness matrix, respectively, and X will be called the state displacement vector. Corresponding to Eq. (20), there is an adjoint differential equation

$$-A^T \dot{Y} + B^T Y = F^* \quad (22)$$

where the adjoint state displacement vector Y and adjoint state force vector F^* are given by

$$Y = \begin{Bmatrix} \dot{y} \\ y \end{Bmatrix}, \quad F^* = \begin{Bmatrix} 0 \\ f^* \end{Bmatrix} \quad (23)$$

Let the complex spectrum matrix be denoted by Λ . (Λ will be diagonal, with the $2n$ eigenvalues λ_i on the principal diagonal. Exceptions in which the eigensystem is defective and Λ has Jordan form include systems with rigid-body modes. Such cases are discussed in Ref. [16].) Let the right complex mode matrix, whose columns are the right eigenvectors, be denoted by Φ , and the left complex mode matrix, whose columns are the left eigenvectors, be denoted by Ψ . Then,

$$\begin{aligned} B\Phi &= -A\Phi\Lambda \\ \Psi^T B &= -\Lambda\Psi A \end{aligned} \quad (24)$$

The right complex mode matrix Φ and left complex mode matrix Ψ may be partitioned in the following manner:

$$\Phi = [\Phi_r \ \Phi_f], \quad \Psi = [\Psi_r \ \Psi_f] \quad (25)$$

where subscripts r and f denote the rigid-body mode partition and the flexible complex modes partition, respectively. Then,

$$\begin{bmatrix} \Psi_r^T \\ \Psi_f^T \end{bmatrix} A [\Phi_r \ \Phi_f] = \begin{bmatrix} \bar{A}_{rr} & 0 \\ 0 & \bar{A}_{ff} \end{bmatrix} \quad (26)$$

where

$$\bar{A}_{rr} = \Psi_r^T A \Phi_r, \quad \bar{A}_{ff} = \Psi_f^T A \Phi_f \quad (27)$$

If there are no repeated eigenvalues, \bar{A}_{ff} is a diagonal matrix. However, \bar{A}_{rr} will not necessarily be diagonal. An equation for B similar to Eq. (26) gives

$$\bar{B}_{rr} = \Psi_r^T B \Phi_r, \quad \bar{B}_{ff} = \Psi_f^T B \Phi_f \quad (28)$$

For damped systems, a right projection matrix P is defined such that if a state displacement vector X is premultiplied by P^T , the rigid-body modes will be removed from the vector. It follows from this definition that

$$P^T [\Phi_r \ \Phi_f] = [0 \ \Phi_f] \quad (29)$$

In Ref. [15] it is shown that

$$P^T = I - \Phi_r \bar{A}_{rr}^{-1} \Psi_r^T A \quad (30)$$

In a similar manner, a left projection matrix Q may be defined such that

$$Q^T [\Psi_r \ \Psi_f] = [0 \ \Psi_f] \quad (31)$$

Then Q will be of the following form

$$Q = I - A \Phi_r \bar{A}_{rr}^{-1} \Psi_r^T \quad (32)$$

The projection matrices defined by Eqs. (30) and (32) can be employed to define *state inertia-relief attachment modes*. To define the attachment modes, first let F_b be the $(2n \times n_b)$ matrix of the state forces with unit forces applied at each boundary coordinate. That is

$$F_a = \begin{bmatrix} 0_{ib} \\ 0_{bb} \\ \dots \\ 0_{ib} \\ I_{bb} \end{bmatrix} = \begin{bmatrix} 0_{ie} & 0_{ir} \\ 0_{ee} & 0_{er} \\ 0_{re} & 0_{rr} \\ \dots & \dots \\ 0_{ie} & 0_{ir} \\ I_{ee} & 0_{er} \\ 0_{re} & I_{rr} \end{bmatrix} \quad (33)$$

Then, let $\hat{\Phi}_a$ be the matrix of static state displacement vectors of a component loaded by QF_a and supported on a user-defined r set of boundary freedoms that provide restraint against rigid-body motion. Let a pseudoflexibility matrix D be defined by

$$D = \begin{bmatrix} -m^{-1} & \vdots & 0 & 0 & 0 \\ \dots & \dots & \dots & \dots & \dots \\ 0 & \vdots & \begin{bmatrix} k_{ii} & k_{ie} \end{bmatrix}^{-1} & 0 \\ 0 & \vdots & \begin{bmatrix} k_{ei} & k_{ee} \end{bmatrix} & 0 \\ 0 & \vdots & 0 & 0 & 0 \end{bmatrix} \quad (34)$$

where it is assumed that m is nonsingular. Then, $\hat{\Phi}_a$ is given by

$$\hat{\Phi}_a = DQF_a \quad (35)$$

To remove the rigid-body modes from $\hat{\Phi}_a$, Eq. (35) may be premultiplied by P^T , leading to the following definition of *right state inertia-relief attachment*

modes:

$$\Phi_a = P^T D Q F_a \quad (36)$$

Reference [15] next defines right and left state residual inertia-relief attachment modes, describes how to couple substructures in state variable form, and provides an example to demonstrate the accuracy of this method for treating systems with general damping.

When the equations of motion of a structure are cast in first-order, state-variable form, as is necessary for the case of general damping such as is treated in Ref. [15], the resulting state equations may be defective. It is shown in Ref. [16] that when the equations of motion of a structure having rigid-body freedom are cast in state-variable form, generalized state rigid-body modes may be required. Reference [16] gives the equations governing these generalized eigenvectors and provides examples for both undamped and damped structures.

3. USE OF LANCZOS VECTORS IN RESPONSE ANALYSIS AND SYSTEM IDENTIFICATION

In Reference [17] an unsymmetric block Lanczos algorithm for structures with general linear damping and with closely-spaced modes is developed. It is also shown that it is possible to identify a Lanczos model from experimental data. Two journal articles based on this work have been written [18,19], and another is in preparation. This Section summarizes this research on unsymmetric block Lanczos methods.

References [17] and [18] show how the equations of motion of a system with arbitrary damping and/or repeated eigenvalues can be solved using an unsymmetric block-Lanczos algorithm. The second-order equation of motion of an n -DOF system

$$m\ddot{x}(t) + c\dot{x}(t) + kx(t) = f(t) \quad (37)$$

is converted to the $2n$ -DOF first-order form

$$A\dot{X}(t) + X(t) = F(t) \quad (38)$$

where X is a state variable having the form

$$X(t) = \left\{ \begin{array}{l} \dot{x}(t) \\ x(t) \end{array} \right\} \quad (39)$$

and A is a $2n \times 2n$ real, non-symmetric matrix.

The dynamic response, $X(t)$, may be approximated by a model order-reduction procedure based on Lanczos vectors as follows. Let a subspace of

right Lanczos vectors be given by

$$\Phi_L^{(p)} = [\Phi_L^{(1)}, \Phi_L^{(2)}, \dots, \Phi_L^{(p)}] \quad (40)$$

and a corresponding subspace of left Lanczos vectors be given by

$$\Psi_L^{(p)} = [\Psi_L^{(1)}, \Psi_L^{(2)}, \dots, \Psi_L^{(p)}] \quad (41)$$

where $\Phi_L^{(j)}$ and $\Psi_L^{(j)}$ are computed by using the following algorithm.

Assume $\Phi_L^{(0)} = \Psi_L^{(0)} = 0$ and select $2n \times r$ blocks of starting vectors $\Phi_L^{(1)}$ and $\Psi_L^{(1)}$, where

$$\Phi_L^{(1)T} \Psi_L^{(1)} = I_{rr}$$

For $j = 1, \dots, (p-1)$, compute

$$M_j = \Psi_L^{(j)T} A \Phi_L^{(j)} \quad (42)$$

$$R_j = A \Phi_L^{(j)} - \Phi_L^{(j)} M_j - \Phi_L^{(j-1)} G_{j-1}^T$$

$$P_j = A^T \Psi_L^{(j)} - \Psi_L^{(j)} M_j^T - \Psi_L^{(j-1)} B_{j-1}^T$$

$$L_j U_j = P_j^T R_j \quad (L-U \text{ decomposition})$$

$$B_j \equiv U_j, \quad G_j \equiv L_j^T$$

$$\Phi_L^{(j+1)} = R_j U_j^{-1}, \quad \Psi_L^{(j+1)} = P_j L_j^{-T}$$

The $2n$ -order model of Eq. (19) may be reduced to $(p \times r)$ -order ($\leq 2n$) through a Ritz-type procedure by letting

$$X(t) = \Phi_L^{(p)} \eta(t) \quad (43)$$

and forming the reduced-order equation of motion

$$A_p \dot{\eta}(t) + \eta(t) = F_p(t) \quad (44)$$

where

$$A_p = \Psi_L^{(p)T} A \Phi_L^{(p)}, \quad F_p = \Phi_L^{(p)T} F(t) \quad (45)$$

Reference [17] shows that A_p can be constructed directly from the M_j , B_j , and G_j matrices computed with Eq. (23).

In Reference [17], reduced-order eigensolution and dynamic response examples based on the above unsymmetric block-Lanczos model order-reduction are given. Figure 2 shows the structure used for the example solutions in Ref. [17]. Due to the lack of space, only selected step response results presented in

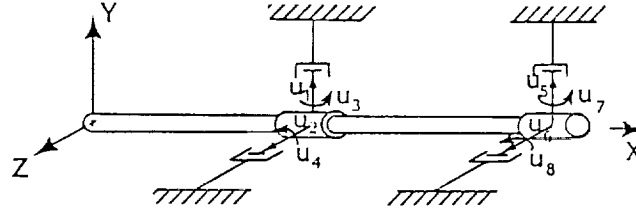


Figure 2: Beam with rotating masses

Ref. [17] will be cited here. The beam in Fig. 2 has eight physical degrees-of-freedom; sixteen state variables. Figures 3a and 3b show the reduced-order response at DOF 5 for unit step inputs at DOFs 5 & 6. Two options for

generating the starting vectors for $\Phi_L^{(1)}$ in Eq. (23) were compared: arbitrary starting vectors, and special starting vectors related to the static displacements. While the special starting vectors led to accurate calculations for a model of order four (Fig. 3b), the arbitrary starting vectors failed to produce accurate results for models of order less than eight.

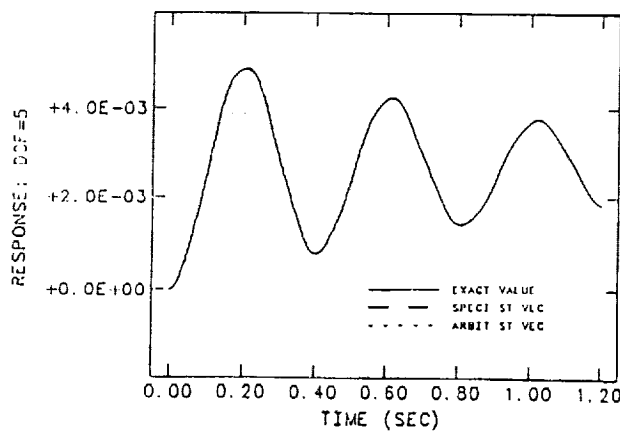


Figure 3a: Unit step response (order=8)

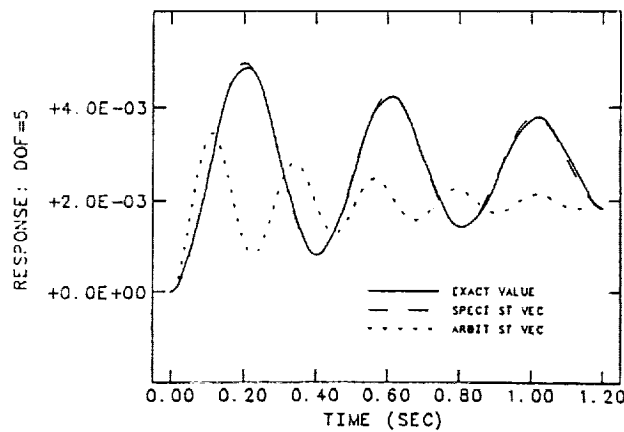


Figure 3b: Unit step response (order=4)

In the block Lanczos algorithm presented above the right and left Lanczos vectors are all theoretically biorthogonal to each other. However, these vectors may lose the biorthogonality due to cancellation and roundoff errors. In a Lanczos-based eigensolver this has been found to result in *ghost* or *spurious* eigenvalues. This problem may be prevented by suitable reorthogonalization and normalization. A strategy for incorporating reorthogonalization and normalization steps in the unsymmetric block Lanczos algorithm is developed in Ref. [17] and is described in Ref. [19].

Mode-superposition based on normal modes is the most commonly used procedure for computing the response of structures to transient type excitation [1]. In many instances it is required that the modal model be validated through experimental modal analysis. The link between analytical modeling based on normal modes and experimental modal analysis has even given rise to the annual International Modal Analysis Conferences (e.g., Ref. [20]) and a companion journal (e.g., Ref. [21]). However, the viewpoint expressed in Refs. [5], [6], [14], and [17] is that mode-superposition based on Krylov vectors (modes) and Lanczos vectors (modes) is an attractive alternative to mode superposition based on normal modes. Hence, Ref. [17] explores the possibility of identifying Lanczos models from experimental data.

Figure 4 shows the proposed system identification procedure which employs a least squares parameter estimation step followed by a Lanczos modeling step. The details of the system identification procedure are contained in Ref. [17], and a journal article on this topic is in preparation. Lanczos system identification was applied to simulated “experimental” data, i.e., time

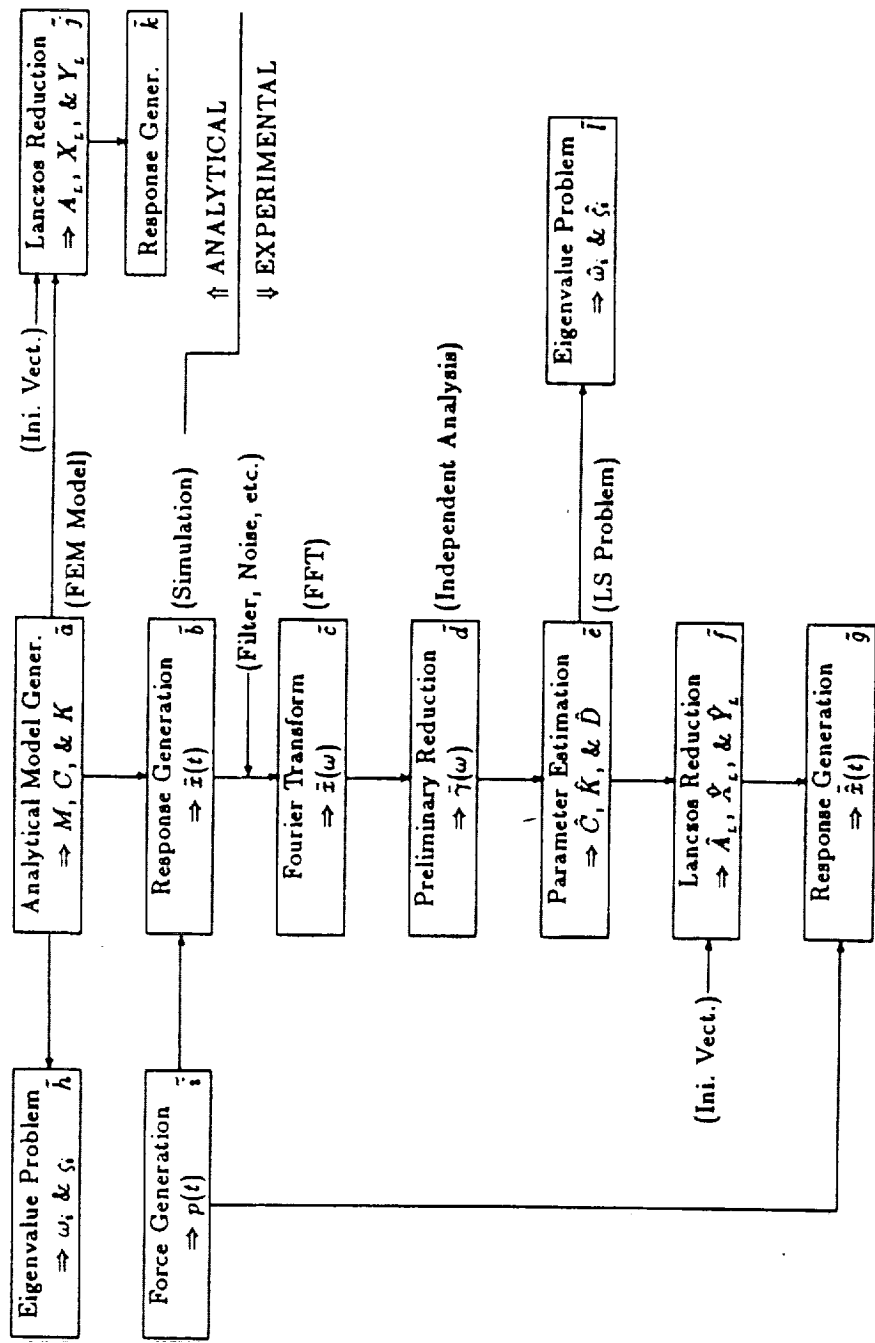


Figure 4: Flow chart for the proposed system identification procedure

histories, for an 8DOF cantilever beam. The system identification procedure, up through and including the parameter estimation and eigenvalue problem steps, was applied to a 60 DOF model of the space station.

Figure 5 shows the 60 DOF finite element model of the equivalent Space Station which was developed in order to apply the proposed system identification procedure to a large space structure (corresponding to the boxes of $\tilde{a} - \tilde{e}$, \tilde{h} , \tilde{i} , and \tilde{l} in Figure 4). Although this model is smaller than the currently proposed Space Station model, it has the same characteristics. This model has modal damping for each mode as well as the rotor mechanism which results in an unsymmetric damping matrix. This model is of order 120 due to the state-vector formulation. The Cray X-MP/24 supercomputer was used for this example.

This structure has an interesting characteristic which can make the model order reduction difficult. Since this model has a very flexible substructure (nodes 6-7-4-9 in Figure 5), which is attached to the main structure (nodes 1-2-3-4-5), the reduced-order model may lose major characteristics of the structure if an order-reduction technique is not applied carefully.

First, an analytical model was generated based on the finite element modeling procedure. Response (acceleration) data were produced by numerical simulation; random input was applied at node number 4 (all six DOFs), the sampling rate was 10Hz, the cut-off frequency was 3.906Hz, the frequency resolution was 0.0195Hz, and the number of samples was 512. The 256-point spectra were produced by the fast Fourier transform, but only 200-point spectra were saved for the next procedure.

By the parameter estimation procedure, nineteen frequencies and damping factors lower than the cut-off frequency were identified in the presence of closely-spaced modes (see Table 1). It was found to be necessary to use a pre-filter, that is an anti-aliasing filter, before the Fourier transform. Three least-squares algorithms were evaluated. The QR decomposition method and the singular value decomposition method gave the same good results, while the normal equation method failed in some cases.

With random noise, which was added to the force and response time histories, the parameter estimation method worked well up to 15% rms (root-mean-square) noise-to-signal ratio.

This example shows that the proposed system identification method (see Figure 4) can be applied to large space structures, although further research is required on the application of Lanczos order-reduction for large size problems.

In summary, a Lanczos algorithm has been developed for systems with arbitrary linear damping and applied both to reduced-order modeling for dynamic response analysis and to experimental system identification.

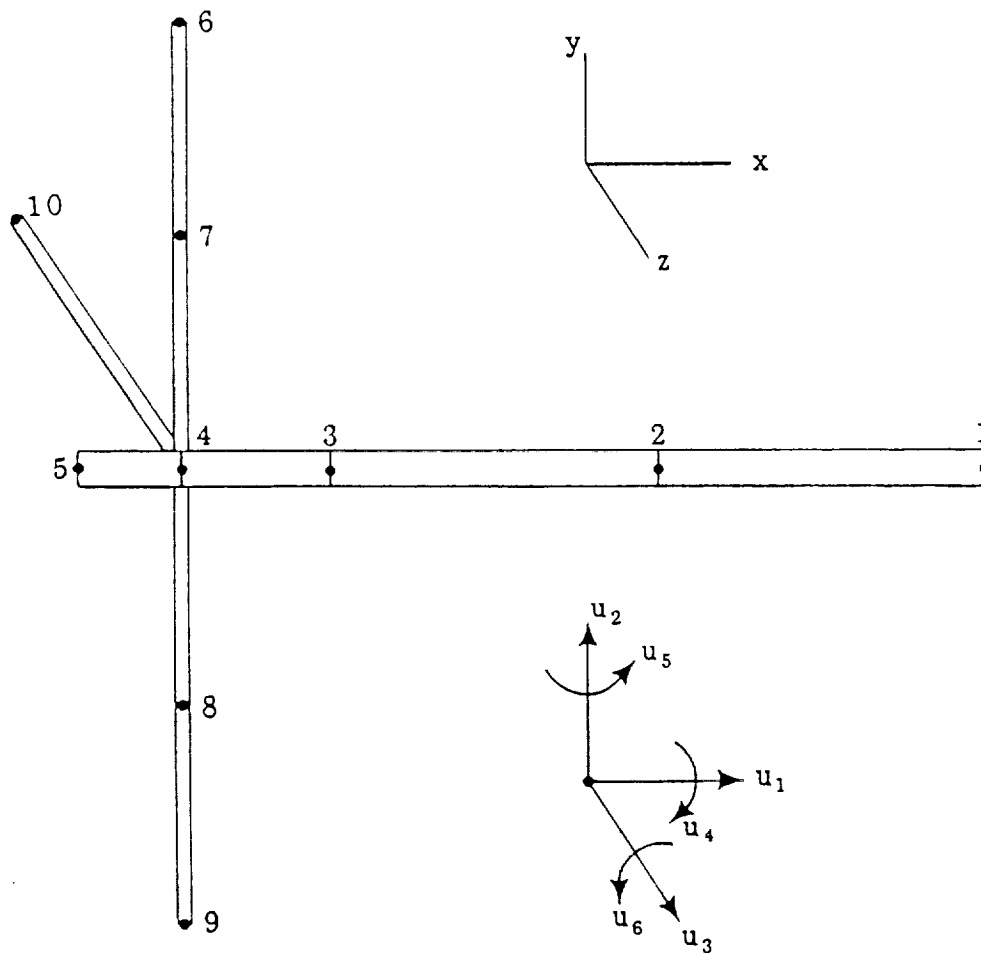


Figure 5: 60-DOF Space Station model

No.	Exact		Identified	
	Frequency	Damping	Frequency	Damping
1	0.105543	0.02000	0.105588	0.01997
2	0.109439	0.02000	0.109360	0.01982
3	0.110349	0.02000	0.110421	0.02011
4	0.126782	0.02000	0.126585	0.02003
5	0.138438	0.02000	0.138640	0.02017
6	0.186127	0.02000	0.186528	0.01956
7	0.681877	0.02000	0.683791	0.02049
8	0.684928	0.02000	0.686575	0.02055
9	0.841581	0.02000	0.844624	0.02034
10	0.846896	0.02000	0.845398	0.02038
11	1.01619	0.02000	1.01416	0.02013
12	1.24198	0.02000	1.25047	0.02106
⋮	⋮	⋮	⋮	⋮

Table 1: Exact and identified eigenvalues

4. APPLICATION OF KRYLOV VECTORS AND LANCZOS VECTORS TO THE CONTROL OF FLEXIBLE STRUCTURES – PART 1

Several studies have been conducted to determine possible application of Krylov vectors and Lanczos vectors to the control of flexible structures. These include Refs. [22] and [23] which develop Lanczos modes for continuous systems (i.e., partial differential equation models of structures) and explore frequency response solutions and transient response solutions based on Lanczos vectors. References [24] through [26] develop Krylov model-reduction methods for undamped and damped structures, describe several interesting features of Krylov reduced-order models, and develop LQ (Linear Quadratic) controller design methods based on Krylov models. This Section summarizes the material covered in Refs. [22] and [23], while Section 5 summarizes the work presented in Refs. [24] through [26].

Previous work on Krylov vectors and Lanczos vectors (e.g., Ref. [6]) has treated only finite degree of freedom systems, generally finite element models of structures. In Ref. [22] Lanczos modes based on continuous models of structures are defined. Lanczos modes (functions) are developed for the cantilever rod shown in Figure 6.

The equation of motion and boundary conditions of the rod in Figure 6 can be written in the following nondimensional form:

$$\frac{\partial^2 u}{\partial x^2} + p(x, t) = \frac{\partial^2 u}{\partial t^2} \quad (46)$$

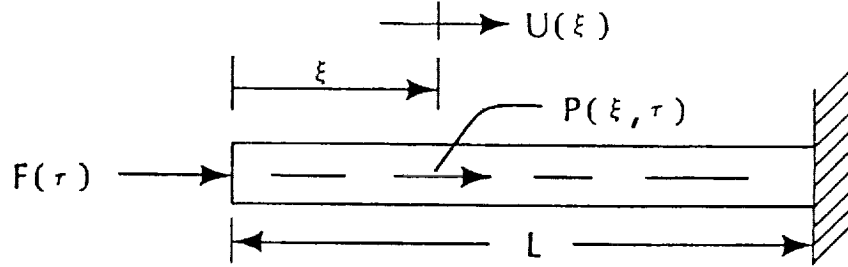


Figure 6: Continuous model of a uniform rod

$$u(1, t) = 0 \quad (47a)$$

$$\frac{\partial u}{\partial x} \Big|_{x=0} = -f(t) \quad (47b)$$

The algorithm presented by Nour-Omid and Clough [6] for finite element models suggests a similar derivation for continuous systems. The algorithm to compute the continuous Lanczos mode $q_{j+1}(x)$ may be expressed by the following sequence of equations:

$$-\bar{r}_j'' = q_j, \quad \bar{r}_j(1) = \bar{r}_j'(0) = 0 \quad (48)$$

$$r_j = \bar{r}_j - \alpha_j q_j - \beta_j q_{j-1} \quad (49)$$

where

$$\alpha_j = \int_0^1 q_j \bar{r}_j dx \quad (50a)$$

$$\beta_j = \left(\int_0^1 r_{j-1}^2 dx \right)^{1/2} \quad (50b)$$

$$q_{j+1} = \left(\frac{1}{\beta_{j+1}} \right) r_j \quad (51)$$

and

$$\beta_{j+1} = \left(\int_0^1 r_j^2 dx \right)^{1/2} \quad (52)$$

To start the computation of Lanczos modes, q_0 and q_1 are required. First, let

$$q_0(x) = 0 \quad (53)$$

As noted by Nour-Omid and Clough, the Lanczos algorithm is particularly advantageous when the force distribution is constant and only the amplitude varies. Here, it is assumed that the force (e.g., control force) is applied only at the tip of the bar, i.e., at $x = 0$. Thus, $q_1(x)$ may be determined by applying a unit (nondimensionalized) force at the free end as shown in Figure 7.

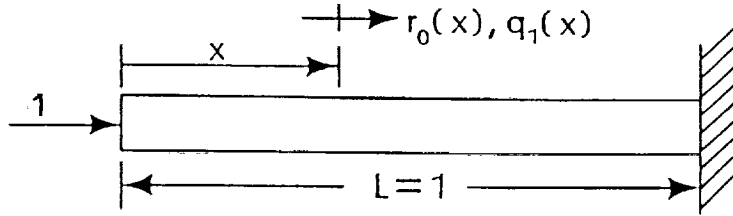


Figure 7: Loading of nondimensionalized rod for Lanczos mode 1

Then, based on Eqs. (46) and (47a)

$$-r_0''(x) = 0$$

$$\begin{aligned}
r_0(1) &= 0 \\
r_0'(0) &= -1 \\
q_1(x) &= (1/\beta_1)r_0(x)
\end{aligned}$$

where

$$\beta_1 = \int_0^1 r_0^2 dx$$

As shown in Ref. [20], this leads to the following normalized Lanczos modes:

$$\begin{aligned}
q_1(x) &= \sqrt{3}(1-x) \\
q_2(x) &= 6.61438x^3 - 19.84313x^2 + 15.87451x - 2.64575 \\
q_3(x) &= -26.11842x^5 + 130.5921x^4 - 232.16374x^3 \\
&\quad + 174.1228x^2 - 49.74937x + 3.31662 \\
q_4(x) &= 103.84437x^7 - 726.91056x^6 + 2012.9831x^5 \\
&\quad - 2795.80986x^4 + 2033.31626x^3 - 731.99386x^2 \\
&\quad + 108.44353x - 3.87298
\end{aligned} \tag{54}$$

These continuous Lanczos modes are plotted in Figures 8a through 8d.

References [22] and [23] discuss some of the typical measures of effectiveness of a dynamic model – frequency response, response to impulse excitation, and response to step excitation. Figures 9a and 9b illustrate typical results of the comparison of responses of reduced-order systems based on normal modes with responses based on Lanczos modes. From responses like those illustrated in Figure 9 it was concluded that Lanczos models provide accurate modeling of low-order system poles and that the system zeros of a Lanczos model are more accurate than the system zeros based on a normal mode model.

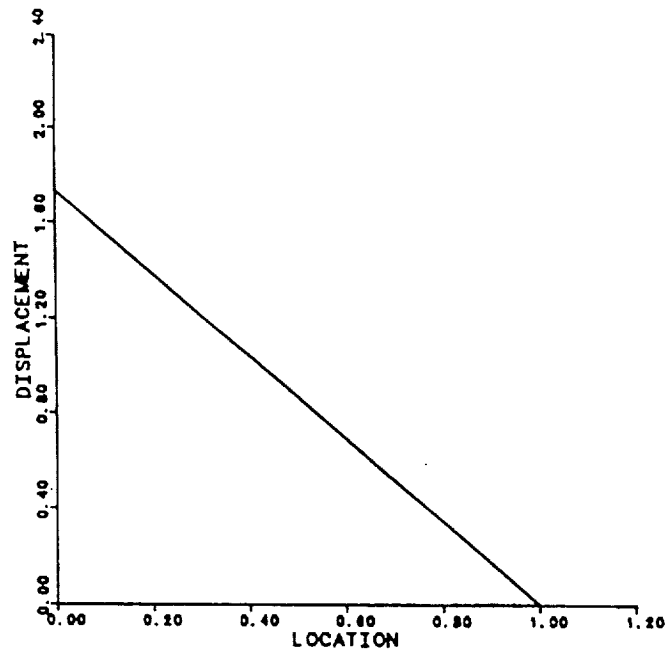


Figure 8a: First continuous Lanczos mode

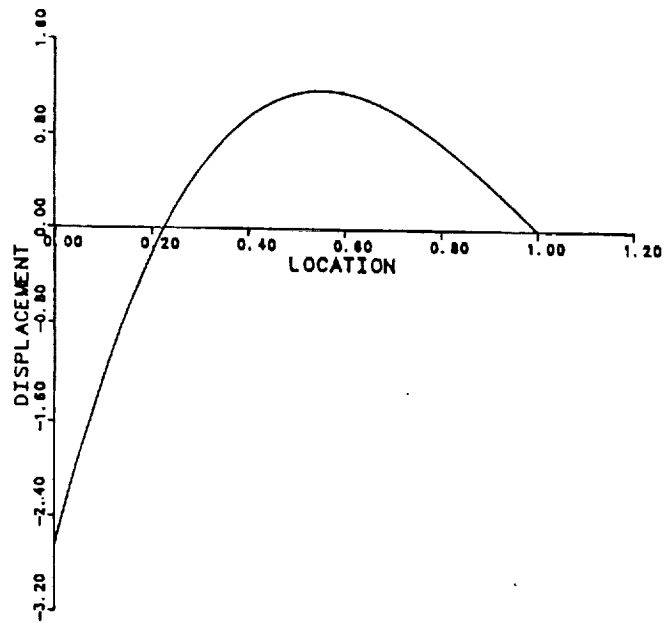


Figure 8b: Second continuous Lanczos mode

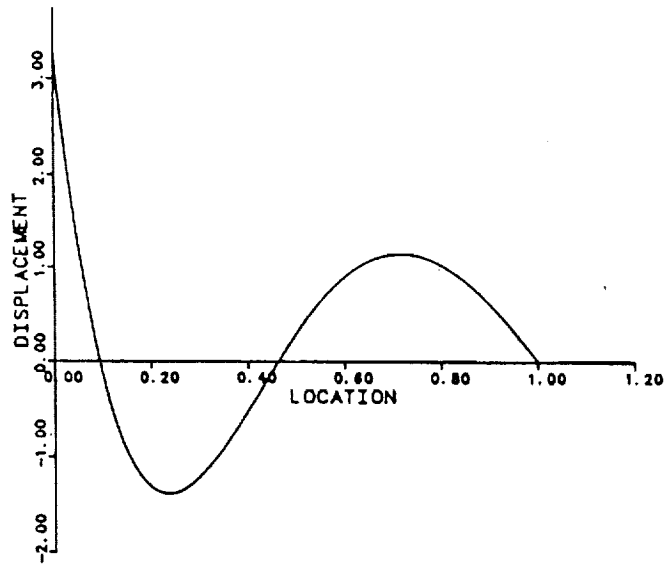


Figure 8c: Third continuous Lanczos mode

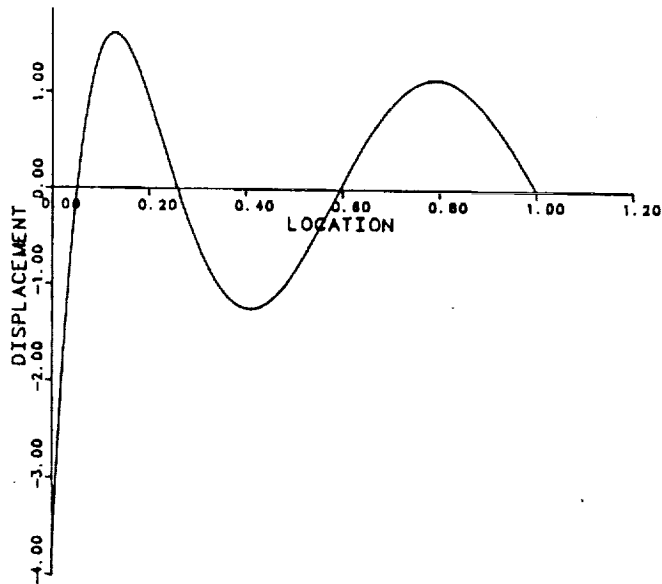


Figure 8d: Fourth continuous Lanczos mode

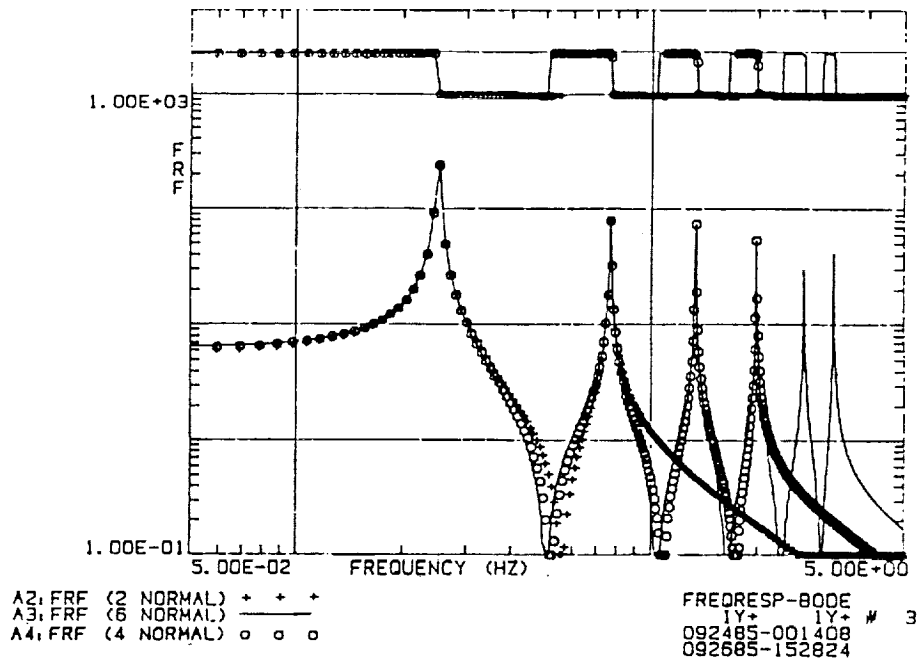


Figure 9a: FRF's based on finite element normal modes

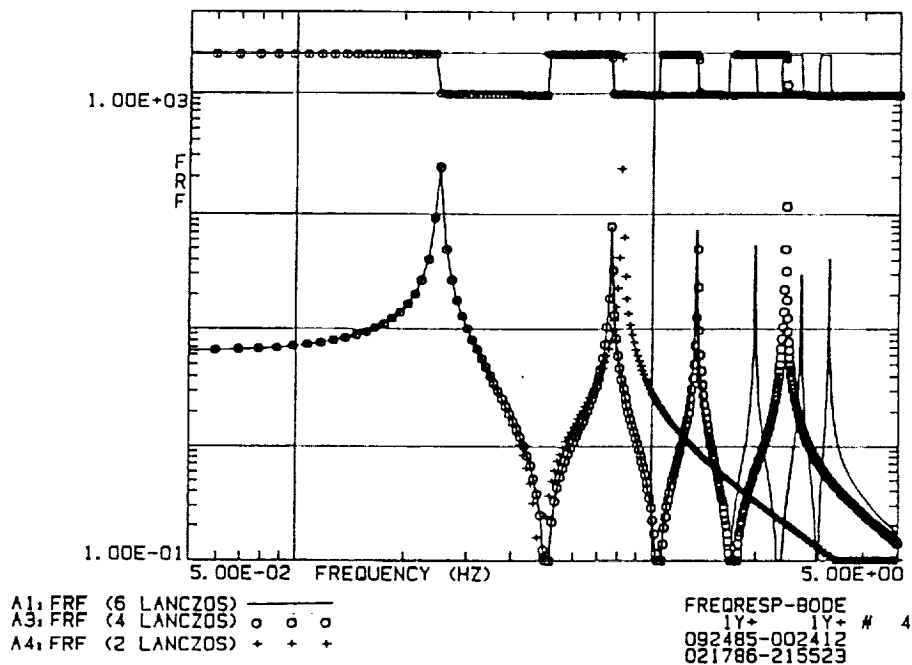


Figure 9b: FRF's based on finite element Lanczos modes

5. APPLICATION OF KRYLOV VECTORS AND LANCZOS VECTORS TO THE CONTROL OF FLEXIBLE STRUCTURES – PART 2

This Section summarizes the work presented in Refs. [24] through [26], in which Krylov vectors and the concept of parameter-matching are combined together to develop Krylov model reduction algorithms for structural dynamics systems. Parameter-matching is a class of well known model reduction methods for general linear time-invariant systems described either by transfer functions or by the first-order state-space form. Krylov model reduction extends the parameter-matching idea to a structural dynamics system described by a second-order matrix differential equation together with an output measurement equation. The reduced-order model obtained by the Krylov model reduction algorithm matches a certain number of system parameters called *low-frequency moments*. For a general linear time-invariant system described by

$$\begin{aligned}\dot{z} &= Az + Bu \\ y &= Cz\end{aligned}\tag{55}$$

the low-frequency moments are defined by $CA^{-i}B$, $i = 1, 2, \dots$, which are the coefficient matrices in the Taylor series expansion of the system transfer function. By matching the low-frequency moments, the Krylov reduced model approximates the lower natural frequency range of the full-order structure. For control applications, it is shown that the Krylov formulation can eliminate the control and observation spillovers, but dynamic spillover needs to be considered.

A Krylov model reduction algorithm for undamped structural dynamics systems is developed in Refs. [25] and [26]. An undamped structural dynamics system is described by the input-output form

$$\begin{aligned} M\ddot{x} + Kx &= Pu \\ y &= Vx + W\dot{x} \end{aligned} \quad (56)$$

Applying the Fourier transform to Eq. (56) and assuming that the system has no rigid-body motion, the system output frequency response function can be expanded around $\omega = 0$ into a Taylor series expansion

$$Y(\omega) = \sum_{i=0}^{\infty} [V(K^{-1}M)^i K^{-1}P + j\omega W(K^{-1}M)^i K^{-1}P] \omega^{2i} U(\omega) \quad (57)$$

In the above expressions, $V(K^{-1}M)^i K^{-1}P$ and $W(K^{-1}M)^i K^{-1}P$ play roles similar to that of the low-frequency moments in the first-order state-space formulation. Therefore, the low-frequency moments of an undamped structural dynamics system described by Eq. (56) are defined by $V(K^{-1}M)^i K^{-1}P$ and $W(K^{-1}M)^i K^{-1}P$, for $i = 0, 1, 2, \dots$

In Refs. [24] and [26] there is a theorem which states that if a projection matrix L is chosen such that $\text{span}\{L\} = \text{span}\{L_P \ L_V \ L_W\}$ with

$$\begin{aligned} L_P &= [K^{-1}P, (K^{-1}M)K^{-1}P, \dots, (K^{-1}M)^p K^{-1}P] \\ L_V &= [K^{-1}V^T, (K^{-1}M)K^{-1}V^T, \dots, (K^{-1}M)^q K^{-1}V^T] \\ L_W &= [K^{-1}W^T, (K^{-1}M)K^{-1}W^T, \dots, (K^{-1}M)^s K^{-1}W^T] \end{aligned}$$

for $p, q, s \geq 0$, then the reduced-order model

$$\begin{aligned} \bar{M}\ddot{\bar{x}} + \bar{K}\bar{x} &= \bar{P}u & \bar{x} \in R^r \quad (r < n) \\ y &= \bar{V}\bar{x} + \bar{W}\dot{\bar{x}} \end{aligned} \quad (58)$$

with $x = L\bar{x}$ and $\bar{M} = L^T M L$, $\bar{K} = L^T K L$, $\bar{P} = L^T P$, $\bar{V} = V L$, and $\bar{W} = W L$, matches the low frequency moments $V(K^{-1}M)^i K^{-1}P$ for $i = 0, 1, \dots, p + q + 1$ and $W(K^{-1}M)^i K^{-1}P$, for $i = 0, 1, 2, \dots, p + s + 1$. Based on that theorem, the following algorithm is developed to generate a Krylov basis which can produce a reduced-order model with the stated parameter-matching property.

Krylov/Lanczos Algorithm

(1) *Starting vector:*

(a) $Q_0 = 0$

(b) $R_0 = K^{-1}\bar{P}$, $\bar{P} = \text{linearly-independent portion of } [P \ V^T \ W^T]$

(c) $R_0^T K R_0 = U_0 \Sigma_0 U_0^T$ (singular-value decomposition)

(d) $Q_1 = R_0 U_0 \Sigma_0^{-\frac{1}{2}}$ (normalization)

(2) *For $j = 1, 2, \dots, k - 1$, repeat:*

(e) $\bar{R}_j = K^{-1} M Q_j$

(f) $R_j = \bar{R}_j - Q_j A_j - Q_{j-1} B_j$ (orthogonalization)

$$A_j = Q_j^T K \bar{R}_j, \quad B_j = U_{j-1} \Sigma_{j-1}^{\frac{1}{2}}$$

(g) $R_j^T K R_j = U_j \Sigma_j U_j^T$ (singular-value decomposition)

(h) $Q_{j+1} = R_j B_{j+1}^{-T} = R_j U_j \Sigma_j^{-\frac{1}{2}}$ (normalization)

end

(3) *Form the k -block projection matrix $L = [Q_1 \ Q_2 \ \dots \ Q_k]$.*

The above algorithm is a Krylov algorithm because the L matrix is generated by a Krylov recurrence formula (Step (e)). It is a Lanczos algorithm

The formulation starts out with an equivalent first-order form of the above equation

$$\begin{aligned} \begin{bmatrix} D & M \\ M & 0 \end{bmatrix} \begin{Bmatrix} \dot{x} \\ \ddot{x} \end{Bmatrix} + \begin{bmatrix} K & 0 \\ 0 & -M \end{bmatrix} \begin{Bmatrix} x \\ \dot{x} \end{Bmatrix} &= \begin{Bmatrix} P \\ 0 \end{Bmatrix} u \\ y = [V \ W] \begin{Bmatrix} x \\ \dot{x} \end{Bmatrix} \end{aligned} \quad (61)$$

Then, the low-frequency moments for the above system are found to be

$$T_i = (-1)^i [V \ W] \begin{bmatrix} -K^{-1}D & -K^{-1}M \\ I & 0 \end{bmatrix}^{i-1} \begin{Bmatrix} K^{-1}P \\ 0 \end{Bmatrix}$$

This suggests the following recurrence formula

$$\begin{Bmatrix} Q_{j+1}^d \\ Q_{j+1}^v \end{Bmatrix} = \begin{bmatrix} -K^{-1}D & -K^{-1}M \\ I & 0 \end{bmatrix} \begin{Bmatrix} Q_j^d \\ Q_j^v \end{Bmatrix} \quad (62)$$

for generating a Krylov subspace for model reduction. Based on the above recurrence procedure, a Krylov model reduction algorithm for damped systems is established.

A plane truss structure with 48 degrees-of-freedom (see Figure 11) was used to illustrate the efficacy of the proposed methods. The structure has a force actuator at f and a displacement sensor at d . The structure geometry is designed to provide closely-spaced eigenvalues. The damping matrix is a generalized proportional damping matrix such that modes 1 to 5 have a 3% damping ratio, modes 6 to 10 have a 5% damping ratio, and the remaining higher modes have successively higher damping. Three reduced-order models are compared: a reduced-order model obtained by using eight damped Krylov vectors, a reduced-order model obtained by using eight undamped

Krylov vectors, and a reduced-order model obtained by retaining eight normal modes. Figures 12 to 14 compare the accuracy of the impulse response of the three reduced-order models. It is seen that for this example the normal mode reduced model and the damped Krylov reduced model have about the same accuracy, while the undamped Krylov reduced model is poor. Therefore, for damped systems, damping effects must be taken into consideration in generating a Krylov reduced model.

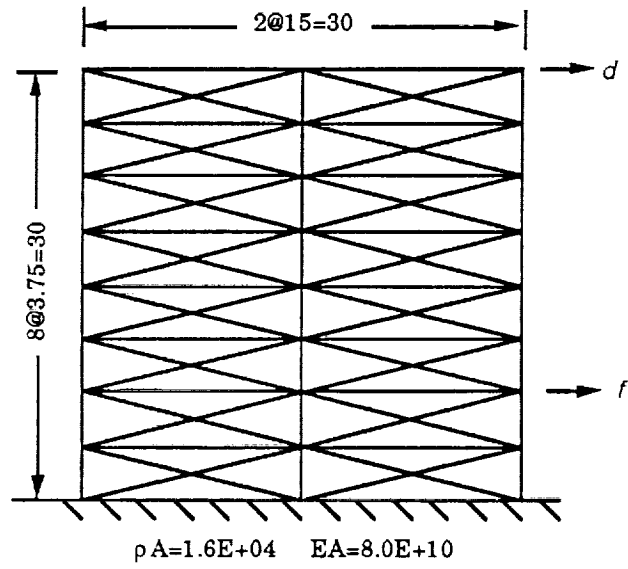


Figure 11: Details of plane truss structure for model reduction example

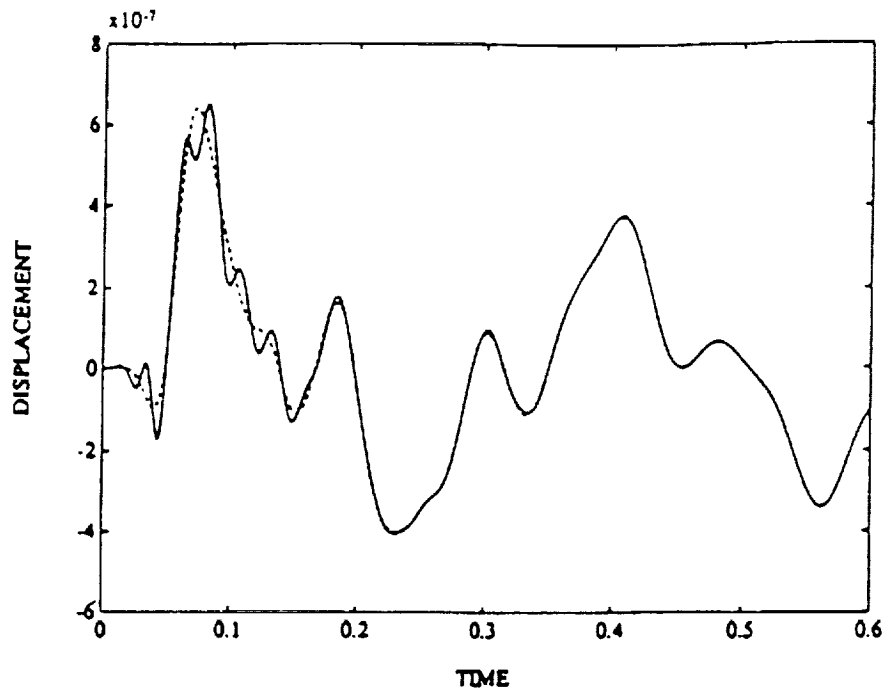


Figure 12: Impulse response; eight normal modes and exact solution

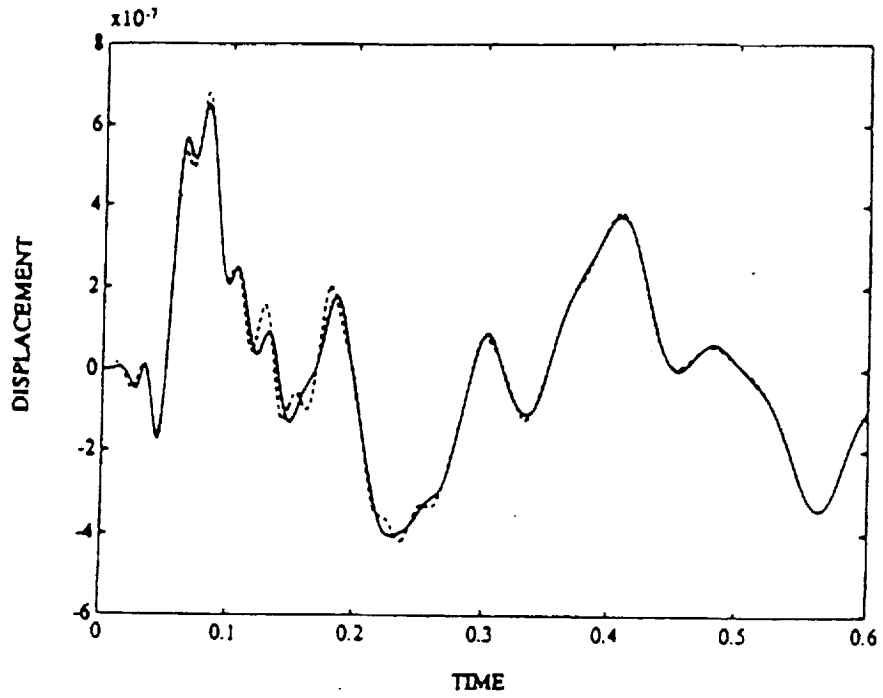


Figure 13: Impulse response; eight damped Krylov modes and exact solution

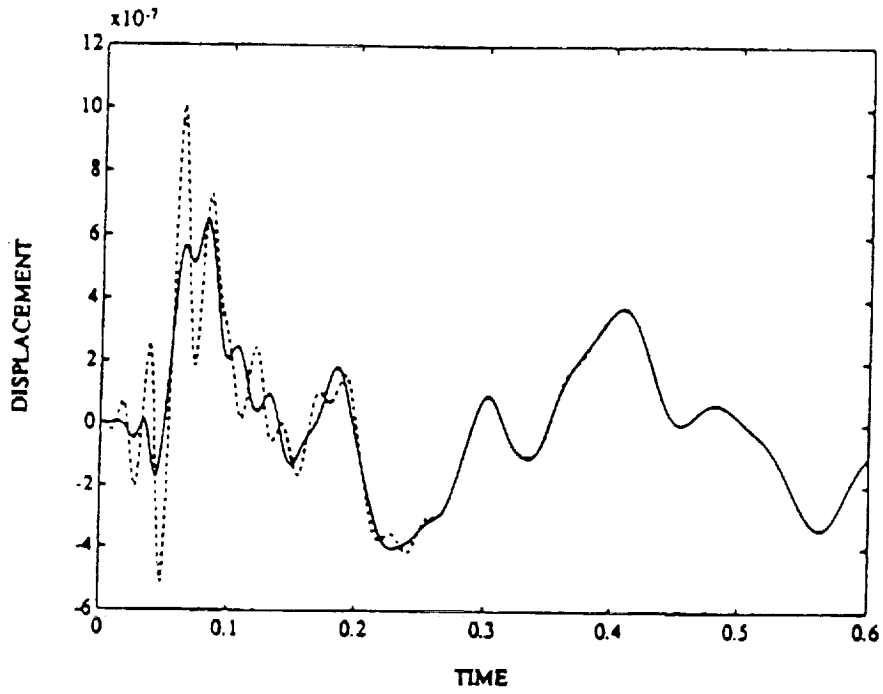


Figure 14: Impulse response; eight undamped Krylov modes and exact solution

In the control of flexible structures, it is shown that there generally exist three types of control energy spillover: *control spillover*, *observation spillover*, and *dynamic spillover*. Figure 15 illustrates the characteristics of spillover. The spillover of control energy is a direct result of model reduction. The com-

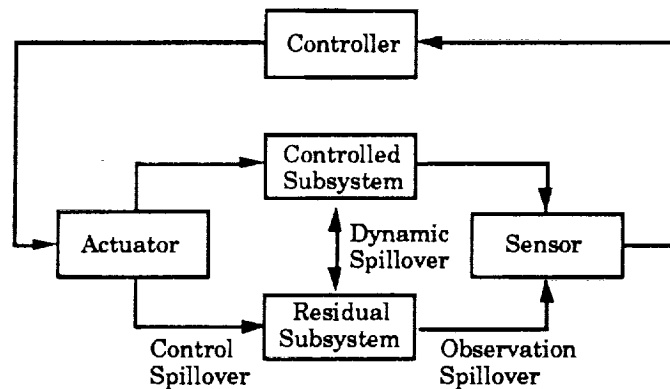


Figure 15: Characteristics of spillover

bined effect of the three types of spillover usually degrades the performance of the controller and sometimes can destabilize the closed-loop system. The conventional normal mode formulation for the control of flexible structures can eliminate dynamic coupling, but it produces both control and observation spillover. If model reduction and control design are based on the system equation described in Krylov coordinates, then the control and observation spillover terms can be eliminated while leaving only the dynamic spillover to be considered. This is the major difference between the Krylov formulation for structural control design and the commonly used normal mode approach.

Several structural control examples are provided in Refs. [24] and [26] to show the superiority of the Krylov method over the normal mode method. One of the examples is a 20 degree-of-freedom lightly-damped truss structure as shown in Figure 16. The structure is reduced to lower-order models by using either Krylov modes or normal modes. Based on each reduced-order model, an LQG control design is carried out to obtain a reduced-order controller. Closed-loop stability of different controllers is compared in Table 2, in which K2 stands for the controller designed based on the 2nd-order Krylov reduced model, N2 stands for the controller designed based on the 2nd-order normal mode reduced model, and so on. It is seen that controllers designed using normal mode reduced models are more likely to cause closed-loop instability than controllers designed using Krylov reduced models. Figure 17 shows that the Krylov-based controllers have better performance than the controllers based on normal mode reduced models.

In summary, Krylov vectors and the concept of parameter-matching are combined together to develop model reduction algorithms for structural dynamics systems. The Krylov formulation for control of flexible structures permits elimination of control and observation spillovers while leaving only dynamic coupling.

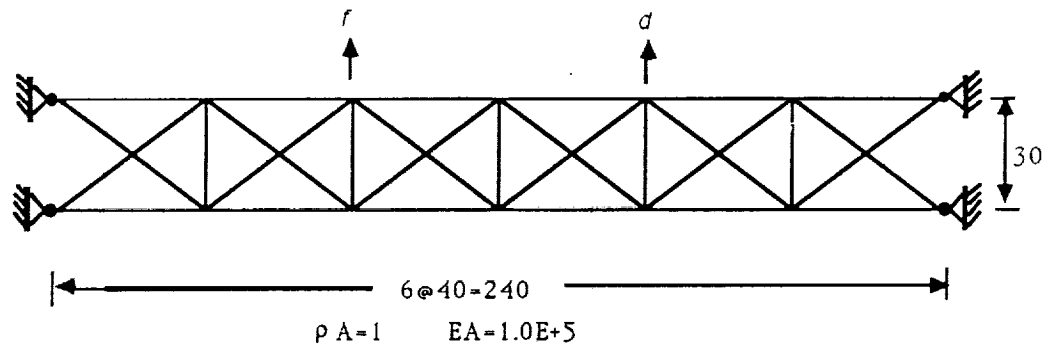


Figure 16: Details of plane truss for control example

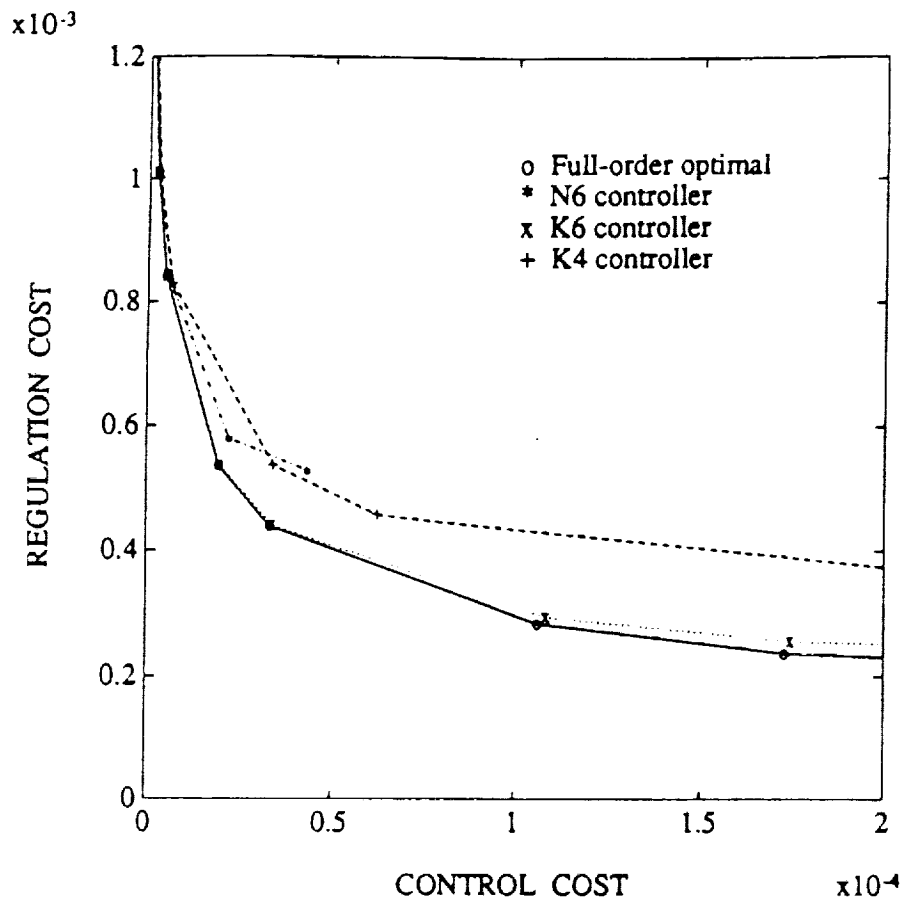


Figure 17: Performance plot

Table 2: Stability of the controllers

Controller	$\rho=.05$	0.1	0.5	1.0	5.0	10.0	50.0	100.0	500.0
K2	U	U	U	U	S	S	S	S	S
K4	U	S	S	S	S	S	S	S	S
K6	S	S	S	S	S	S	S	S	S
K8	U	S	S	S	S	S	S	S	S
K10	S	S	S	S	S	S	S	S	S
N2	U	U	U	U	U	U	S	S	S
N4	U	U	U	U	U	U	S	S	S
N6	U	U	U	U	S	S	S	S	S
N8	S	S	S	S	S	S	S	S	S
N10	S	S	S	S	S	S	S	S	S

S: the closed-loop system is stable. U: unstable

6. A BILEVEL ARCHITECTURE FOR THE CONTROL OF FLEXIBLE STRUCTURES

Although attachment modes are not employed directly in Ref. [27], the study was conducted to provide background on the topic of control structure interaction and to explore the possibility of developing a substructure-based control system architecture.

In the design of a control system architecture for control of a flexible structure, there are several characteristics that are desirable. The architecture should be physically motivated, meaning that it should be particularly suited to the nature of the structure. The algorithms utilized must not involve an excessive amount of on-line computation as this introduces time delay and promotes the increase of round-off error, both of which may lead to unsatisfactory performance and control instability. The control scheme should be easy to implement in that the amount of hardware required and complexity of the implementation techniques should be minimized. Finally, the scheme should be cost effective, as energy and fuel are not necessarily in abundant supply.

Two levels of control are chosen in the architecture proposed in Ref. [27], such that the upper or global level is a centralized controller whose purpose is to maintain overall structure attitude and shape, and the lower or residual level is a decentralized control whose function is to provide damping augmentation. The global control is based on a reduced structure model which is only large enough to include critical, low-frequency motion associated with

rigid body modes and a few flexible modes. The residual control is necessary to suppress vibration in higher modes which need not be modeled or controlled explicitly. Another reason for the residual control is related to control spillover from the global control which may destabilize the unmodeled vibrational modes. The principal causes for the spillover are modal truncation and inaccurate representation of the actual motion. Thus, since the residual control itself must be extremely stable and robust, direct velocity feedback is employed in the residual control law.

Two examples are presented in Ref. [27] to show that the proposed bilevel control architecture is successful in controlling low-order structures. For these two examples there was little loss in performance and only a slight increase in control cost as compared to full state and full measured-state feedback approaches. The proposed bilevel control architecture appears to be a viable alternative for control of flexible structures.

7. SUMMARY AND RECOMMENDATIONS

This report summarizes extensive research on the application of attachment modes in dynamic response analysis and in control-structure interaction analysis for flexible structures. In particular, methods based on Krylov vectors and Lanczos vectors have been developed and have been shown to be superior to normal mode methods in many cases. Included are block-Krylov methods for substructure analysis, block-Lanczos methods for structures with general damping, and model order-reduction and controller design methods based on Krylov and Lanczos vectors.

Future research should address control theoretic aspects of controller design based on Krylov/Lanczos modes, and substructure-based controller design procedures should be developed.

REFERENCES

1. Craig, R. R. Jr., *Structural Dynamics – An Introduction to Computer Methods*, John Wiley and Sons, Inc., New York, NY, 1981.
2. Bamford, R. M., "A Modal Combination Program for Dynamic Analysis of Structures (Revision No. 1)," *Tech. Memorandum No. 33-290*, Jet Propulsion Laboratory, Pasadena, CA, 1967.
3. Craig, R. R. Jr. and Chang, C. J., "On the Use of Attachment Modes in Substructure Coupling for Dynamic Analysis," *Proc. 18th AIAA/ASME Structures, Structural Dynamics and Materials Conf.*, San Diego, CA, 1977, pp. 89-99.
4. Martinez, D. R. and Gregory, D. L., "A Comparison of Free Component Mode Synthesis Techniques Using MSC/NASTRAN," *Sandia Report SAND83-0025*, 1984.
5. Wilson, E. L., Yuan, M. W., and Dickens, J. M., "Dynamic Analysis by Direct Superposition of Ritz Vectors," *Earthquake Eng. & Struc. Dyn.*, Vol. 10, No. 6, 1982, pp. 813-821.
6. Nour-Omid, B. and Clough, R. W., "Dynamic Analysis of Structures Using Lanczos Co-Ordinates," *Earthquake Eng. & Struc. Dyn.*, Vol. 12, No. 4, 1984, pp. 565-577.
7. Craig, R. R. Jr., "A Review of Time-Domain and Frequency-Domain Component Mode Synthesis Methods," *Combined Experimental/*

Analytical Modeling of Dynamic Structural Systems, ASME, AMD-Vol. 67, New York, NY, 1985, pp. 1-30.

8. Craig, R. R. Jr., "A Review of Time-Domain and Frequency-Domain Component Mode Synthesis Methods," *Int. J. Analyt. and Exp. Modal Analysis*, Vol. 2, No. 2, 1987, pp. 59-72.
9. Hurty, W. C., "Dynamic Analysis of Structural Systems Using Component Modes," *AIAA Journal*, Vol. 3, No. 4, 1965, pp. 678-685.
10. Craig, R. R. Jr. and Bampton, M. C. C., "Coupling of Substructures for Dynamic Analysis," *AIAA Journal*, Vol. 7, No. 7, 1968, pp. 1313-1319.
11. MacNeal, R. H., "A Hybrid Method of Component Mode Synthesis," *Computers and Structures*, Vol. 1, No. 4, 1971, pp. 581-601.
12. Rubin, S., "Improved Component-Mode Representation for Structural Dynamic Analysis," *AIAA Journal*, Vol. 13, No. 8, 1975, pp. 995-1006.
13. Benfield, W. A. and Hruda, R. F., "Vibration Analysis of Structures by Component Mode Substitution," *AIAA Journal*, Vol. 9, No. 7, 1971, pp. 1255-1261.
14. Craig, R. R. Jr. and Hale, A. L., "Block-Krylov Component Synthesis Method for Structural Model Reduction," *J. Guidance, Control, and Dynamics*, Vol. 11, No. 6, 1988, pp. 562-570.

15. Craig, R. R. Jr. and Ni, Z., "Component Mode Synthesis for Model Order Reduction of Non-classically-Damped Systems," *AIAA J. Guidance, Control, and Dynamics*, Vol. 12, No. 4, 1989, pp. 577-584.
16. Craig, R. R. Jr., Su, T. J., and Ni, Z., "State Variable Models of Structures Having Rigid-Body Modes," *to appear AIAA J. Guidance, Control, and Dynamics*.
17. Kim, H. M. and Craig, R. R. Jr., "System Identification for Large Space Structures," *Report No. CAR 88-9, Center for Aeronautical Research, The Univ. of Texas at Austin, Austin, TX*, Dec. 1988.
18. Kim, H. M. and Craig, R. R. Jr., "Structural Dynamics Analysis Using an Unsymmetric Block Lanczos Algorithm," *Int. J. Num. Methods in Engr.*, Vol. 26, No. 10, 1988, pp. 2305-2318.
19. Kim, H. M. and Craig, R. R. Jr., "Computational Enhancement of an Unsymmetric Block Lanczos Algorithm," *submitted to Int. J. Num. Methods in Engr.*
20. *Proc. International Modal Analysis Conference*, Union College, Schenectady, NY, and Society for Experimental Mechanics, Inc., Bethel, CT, 1st (1982) – 7th (1989).
21. *Int. J. Analytical and Experimental Modal Analysis*, Society for Experimental Mechanics, Inc., Bethel, CT, Vol. 1(1986) – Vol. 4 (1989).

22. Turner, R. M. and Craig, R. R. Jr., "Use of Lanczos Vectors in Dynamic Simulation," *Report No. CAR 86-3, Center for Aeronautical Research, The Univ. of Texas at Austin, Austin, TX, May 1986.*
23. Craig, R. R. Jr. and Turner, R. M., "Lanczos Models for Reduced-Order Control of Flexible Structures," *Structural Dynamics and Control Interaction of Flexible Structures, Proc. of a workshop held at George C. Marshall Space Flight Center, NASA CP-2467, Part 2, Huntsville, AL, April 22-24, 1986, pp. 999-1012.*
24. Su, T. J. and Craig, R. R. Jr., "Application of Krylov Vectors and Lanczos Vectors to the Control of Flexible Structures," *Report No. CAR 89-2, Center for Aeronautical Research, The Univ. of Texas at Austin, Austin, TX, August 1989.*
25. Su, T. J. and Craig, R. R. Jr., "Model Reduction and Control of Flexible Structures Using Krylov Vectors," *to appear AIAA J. Guidance, Control, and Dynamics. Also Paper No. 89-1237, 30th AIAA/ASME/ASCE/AHS/ASC Structures, Structural Dynamics and Materials Conf., Mobile, AL, April 2-4, 1989.*
26. Su, T. J. and Craig, R. R. Jr., "Krylov Model Reduction Algorithm for Undamped Structural Dynamics Systems," *submitted to AIAA J. Guidance, Control, and Dynamics.*
27. Tave, J. S., Bennighof, J. K., and Craig, R. R. Jr., "A Bilevel Architecture for the Control of Flexible Structures," *Report No. CAR*

*87-2, Center for Aeronautical Research, The Univ. of Texas at Austin,
Austin, TX, July 1987.*

